12WCEE 2000

EFFECTS OF NON PROPORTIONAL DAMPING ON THE SEISMIC RESPONSES OF SUSPENSION BRIDGES

Quan QIN[1] And Lei LOU[2]

SUMMARY

Modern suspension bridges have stiffening steel decks and RC towers. The well separated different materials cause damping to be unevenly distributed for the complete bridge, known as 'non-classical' damping. The equations of motion for such structures are damping coupled in the modal coordinate system. Most commercial dynamic finite element analysis computer programs can not solve these equations. This paper discusses three methods for solving the equations and their implementation in computer programs. The seismic response analyses of the Tsing Ma bridge and Humen bridge indicate that non-classical damping may have a significant influence on the seismic response of suspension bridges.

INTRODUCTION

Modern suspension bridges generally consist of stiffening steel decks, steel main cables, steel hangers and concrete towers. The two materials have clearly different damping properties. The structural components in the two different materials are well separated and this causes suspension bridges to undergo what is known as 'non-classical' damping.

The effect of damping on the dynamic response of structures is significant, although the effect is of less significance than those of the inertial and stiffness properties. The linear viscous damping model is often applied to the dynamic analysis of structures with a damping ratio of 2% for steel structures and 5% for concrete structures.

The damping describes the energy-loss mechanisms. Actual energy-loss mechanisms include friction between different components, friction within materials and forces from environmental media which resist motion. Linear viscous damping is the simplest model as it allowa the equations of motion to be uncoupled. Its energy-loss per cycle, however, depends on the frequency of the applied force, which is contradictory to a great deal of test evidence. Furthermore, the modal linear viscous damping ratio calculated from Rayleigh damping is proportional to the modal frequency. Both induce errors in the analytical response.

Although complex stiffness damping induces energy-loss per cycle which is independent of the applied force frequency, it makes the modal damping ratio (deduced from Rayleigh damping) proportional to the square of the frequency of applied forces. In addition, it induces complex variables in the equations of motion. These two deficiencies limit its application. Some more complicated damping models have been discussed. To date, there is no perfect damping model.

General engineering structures have light damping. The effect of damping on structural responses is much less than effects of inertia and stiffness. It is not worth using complicated damping models for such a small effect.

Linear viscous damping is the most widly used in practice, for general bridges without special damping devices, due to its simplicity.

[1] *Dept. of Civil Engineering, Tsinghua University, Haidian, Beijing, China. Email:qq-dci@mail.tsinghua.edu.cn*
[2] *Dept. of Civil Engineering, Tsinghua University, Haidian, Beijing, China. Email:qq-dci@mail.tsinghua.edu.cn*

The paper discusses the influence of non-classical linear viscous damping on the seismic response of suspension bridges. The Tsing Ma bridge and Humen bridge are taken as examples. The main 1377 m span of the Tsing Ma bridge has a steel truss stiffening deck and two concrete towers. The main 888 m span of the Humen bridge has a steel box deck and two concrete towers. Fig 1 and Fig 2 show the analytical models.

To date only the classical damping model has been used for the response analysis of bridge structures subjected to earthquake and wind loading. The common commercial dynamic finite element analysis computer programs do not allow the equations of motion to be solved with non-classical damping. Initially, the paper discusses three methods to solve the equations of motion with non-classical damping, and then the computer implementation of these methods is discussed. Seismic responses of the two suspension bridges, assuming non-classical damping and classical damping, are discussed and compared in the final section of the paper.

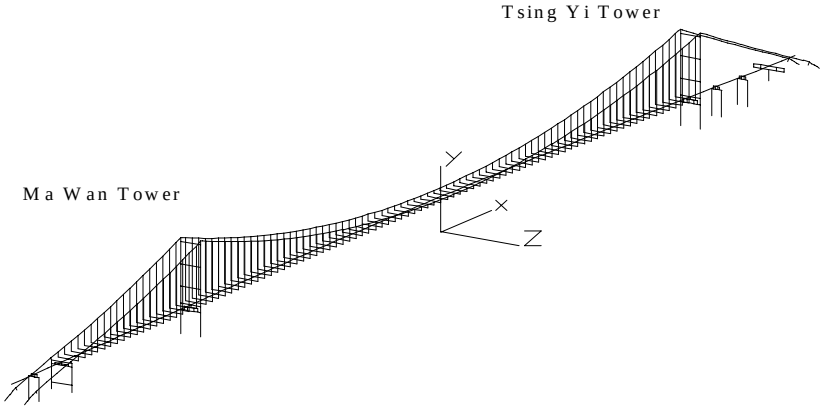

Fig. 1 Tsing Ma Bridge

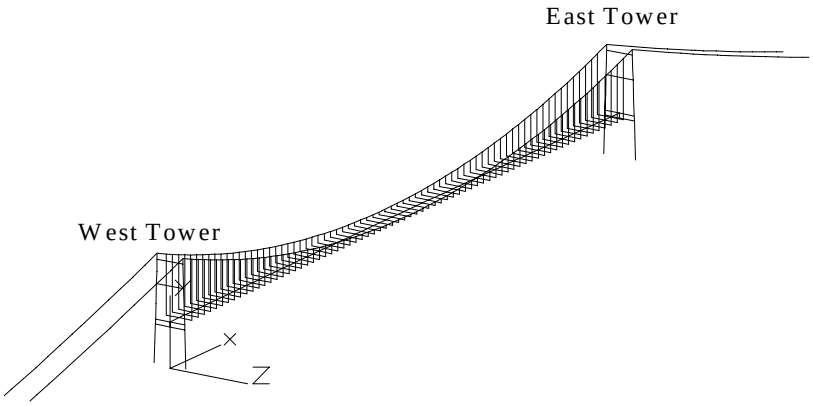

Fig. 2 Humen Bridge

EQUATIONS OF MOTION WITH NON CLASSICAL DAMPING AND SOLUTIONS

For suspension bridges without special dampers it can be assumed that the steel structural parts including the main cables, hangers and stiffening decks exhibit a uniformly distributed 2%, and that the concrete parts, including towers and piers, exhibit a uniformly distributed 5% damping. Consequently, a pair of Rayleigh damping coefficients α_s and β_s can be used to describe the element damping matrices of all steel structural components, and another pair of Rayleigh damping coefficients α_c and β_c can be used to describe the element damping matrices of all concrete structural components.

$$\boldsymbol{c}_s^e = \alpha_s \boldsymbol{m}_s^e + \beta_s \boldsymbol{k}_s^e$$

$$\boldsymbol{c}_c^e = \alpha_c \boldsymbol{m}_c^e + \beta_c \boldsymbol{k}_c^e \qquad (1)$$

where $\boldsymbol{m}_s$ and $\boldsymbol{m}_c$ are the element mass matrices of the steel and concrete components, respectively, $\boldsymbol{k}_s$ and $\boldsymbol{k}_c$ are the element stiffness matrices of the steel and concrete components, and α_s, β_s, α_c and β_c are determined from two selected undamped natural frequencies ω_m and ω_n of the complete bridge system, following [Clough and Penzien, 1993]. Assembling all element damping matrices leads to the combined system non-classical damping matrix C. The equations of motion of the complete system with non-classical damping are

$$\boldsymbol{M}\ddot{\boldsymbol{U}} + \boldsymbol{C}\dot{\boldsymbol{U}} + \boldsymbol{K}\boldsymbol{U} = \boldsymbol{F}(\boldsymbol{x},t) \tag{2}$$

where M and K are the global mass and stiffness matrices. U is the global displacement vector and F is the dynamic load vector. x is the geometric coordinate vector of nodes in the analytical model.

The first method discussed in the paper to solve Eqn 2 is by step-by-step integration in the geometric coordinate system.

Solving the undamped equations of motion of Eqn 2 leads to the first n natural frequencies ω_i, i = 1,…,n and mode shapes Φ_i, i = 1,…,n. Then the displacement vector Y in normal coordinates can represent U

$$\boldsymbol{U} = \boldsymbol{\mu}\boldsymbol{Y} \tag{3}$$

where $\boldsymbol{\mu} = [\boldsymbol{\mu}_1 \boldsymbol{\mu}_2 \ldots \boldsymbol{\mu}_n]$. Substituting Eqn 3 into Eqn 2 pre-multiplying by $\boldsymbol{\mu}^T$ leads to

$$\boldsymbol{m}\ddot{\boldsymbol{Y}} + \bar{\boldsymbol{c}}\dot{\boldsymbol{Y}} + \boldsymbol{k}\boldsymbol{Y} = \boldsymbol{p} \tag{4}$$

where $\boldsymbol{m} = \boldsymbol{\mu}^T \boldsymbol{M} \boldsymbol{\mu}$

$$\bar{\boldsymbol{c}} = \boldsymbol{\mu}^T \boldsymbol{C} \boldsymbol{\mu}$$

$$\boldsymbol{k} = \boldsymbol{\mu}^T \boldsymbol{K} \boldsymbol{\mu} \tag{5}$$

$$\boldsymbol{P} = \boldsymbol{\mu}^T \boldsymbol{F}$$

Here $\bar{\boldsymbol{c}}$ is not diagonal, because in general it does not satisfy the symmetrical conditions developed by [Caughey, 1960]

$$\bar{\boldsymbol{c}} = \boldsymbol{c}_d + \hat{\boldsymbol{c}} \tag{6}$$

where $\boldsymbol{c}_d$ is the diagonal part of $\bar{\boldsymbol{c}}$ and $\hat{\boldsymbol{c}}$ is the off-diagonal part of $\bar{\boldsymbol{c}}$.

The transform, [Foss, 1958], can be used to change Eqn 4 into a first order differential equation system, and the complex mode method can be used to solve it. However, it doubles the number of degrees of freedom and induces damped modes. No commercial computer program uses this method.

The second method to solve Eqn 4 presented in this paper is by step-by-step integration in normal coordinates. Duhamel's integration can not be used here, because Eqn 4 is damping coupled. The two non-conditional stable numerical integration methods, Wilson-θ and Newmark methods are used here. When solving in the normal coordinates, the number of selected modes, n, can be much less than the number of degrees of freedom, N, of the complete system, including only those models which have an impact on the response. The second method, therefore, can be much more efficient than the first one.

The third method, [Claret and Vinancio-Filho, 1991], to solve Eqn 4 moves the off-diagonal part $\hat{\boldsymbol{c}}$ to the right side of Eqn 4 as a pseudo force. So, the third method is called the pseudo force iteration method. After this movement, the left side of Eqn 4 becomes decoupled,

$$\ddot{y}_i + 2\xi_i\omega_i\dot{y}_i + \omega^2{}_i y_i = p_i - \sum_{j=1}^{n}\hat{c}_{ij}\dot{y}_j \quad ,i = 1,\cdots,n \tag{7}$$

where y_i is the ith component of Y, p_i is the ith component of generalized forces, ξ_i is the ith modal damping ratio, $\hat{c}_{ij}$ is the element in the ith row and jth column of $\hat{\boldsymbol{c}}$.

Duhamel's integration can be used to solve the decoupled equations in Eqn 7. In order to speed up the convergence, Eqn 7 can be written in the Gauss-Seidel iteration form

$$\ddot{y}_i^{(k)} + 2\xi_i\omega_i\dot{y}_i^{(k)} + \omega_i^2 y_i^{(k)} = p_i - \sum_{j=1}^{i-1}\hat{c}_{ij}\dot{y}_j^{(k)} - \sum_{j=i+1}^{n}\hat{c}_{ij}\dot{y}_j^{(k-1)} \quad . \; i = 1,\cdots,n \tag{8}$$

The convergence condition is

$$\underset{i}{Max}\left|1 - \frac{\dot{y}_i^{(k-1)}}{\dot{y}_i^{(k)}}\right| \le \varepsilon \tag{9}$$

where ε is a subjective tolerance, a positive constant.

The convergence rate can be measured by the convergent index β

$$\beta \equiv \frac{1}{\left|\sum_{j=1, j\neq i}^{n}\frac{D_{ji}}{\omega_i^2}\hat{c}_{ij}\right|} \tag{10}$$

Where

$$D_{ij} = \frac{1}{\sqrt{\left[1 - \left(\frac{\omega_j}{\omega_i}\right)^2\right]^2 + 4\xi_i^2\left(\frac{\omega_i}{\omega_j}\right)^2}} \tag{11}$$

It is convergent if β >1. The greater β, the faster the convergence.

IMPLEMENTATION AND VALIDATION

When a commercial computer program is selected for adding these three methods of solving the equations with non-classical damping, the following work should be carried out. First, enough space should be added and arranged for storing the element damping matrices and the combined system damping matrix. The combined system damping matrix should be stored in the half-band and blocked form.

Then step-by-step integration in normal coordinates and the pseudo force iteration method are added to a commercial program as subroutines.

In order to make the iteration scheme more efficient, the mode acceleration method, [Ibrahimbegovic and Wilson , 1989] is induced in the subroutine. With the same number of modal components, the mode acceleration method gives more accurate solutions than by the mode displacement method.

The paper uses many examples to validate the subroutines, including the following two.

Example 1 A two DOF system, shown in Fig 3, [Ibrahimbegovic and Wilson, 1989], has masses m1 = m2 =1 kg, spring stiffness' k1 = k2 = 1 kN/m and viscous damping coefficients C2 = 1 s/m and C1 = •C2. A force f(t), shown in Fig 4, is applied to the second mass m2. When a=100, the system has strong non-classical damping. The time histories of the displacement of mass m2 and the force in spring k2, calculated by the subroutines, are shown in Fig 5. In these figures the continuous lines are solutions calculated by the pseudo force method and dotted lines are solutions calculated using step-by-step integration in geometric coordinates, which are taken as exact solutions. From Fig 5 the solutions calculated with the presented methods are exactly the same as those given by [Ibrahimbegovic and Wilson, [1989].

given by [Ibrahimbegovic and Wilson, [1989].

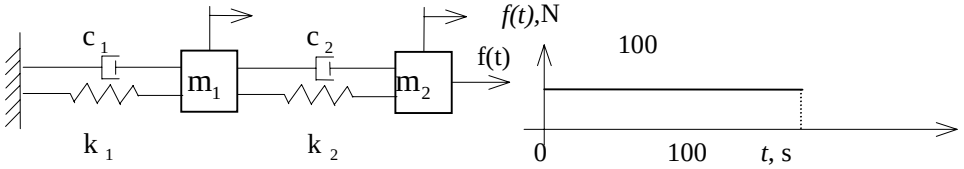

Fig. 3 Two DOF System **Fig. 4 Force *f(t)***

Example 2 The response of the Tsing Ma bridge to the El Centro three component accelerations: Assume that the damping ratio ξ = 2% for the complete bridge. The computer program SAP6 is taken as the basic program to which the three methods presented above are added. The response of the Tsing Ma bridge with classical damping ratio ξ = 2%, is calculated with SAP6. Responses are also calculated with the added subroutines for non-classical damping, but with the damping ratio of 2% taken for both steel and concrete components. The two programs produce the same results over the complete time duration 53.74s. Fig 6 shows the mid span horizontal moment M_z time-history of the steel stiffening deck calculated found from the added subroutine.

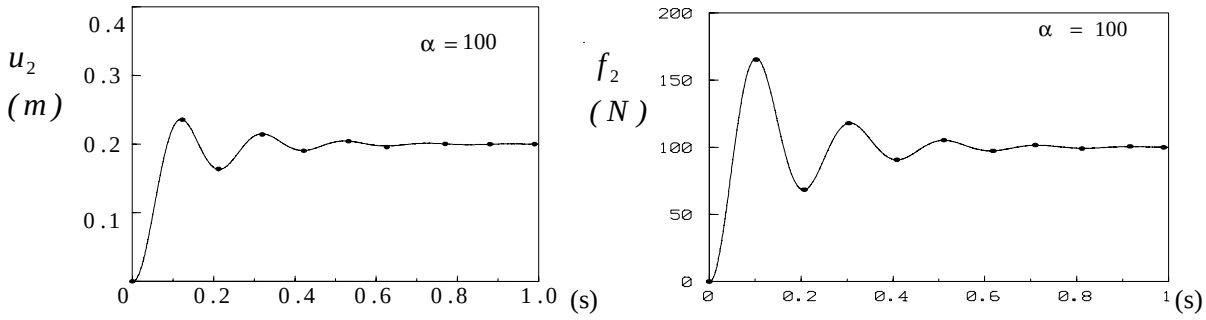

(a) Displacement history of m_2, (m) **(b) Force history in k_2 , (N)**

Fig. 5 Response of 2 DOF System with Non-Classical Damping

SEISMIC RESPONSES OF TSING MA AND HUMEN BRIDGES WITH NON CLASSICAL DAMPING

The damping ratio for the steel stiffening decks, hangers and main cables of the Tsing Ma and Humen bridges is taken as 2%. The damping ratio for the concrete towers and piers of the two bridges is taken as 5%.

The first 140 natural modes of the Tsing Ma bridge are considered, see [Qin, Luo and Sun, 1999]. The first

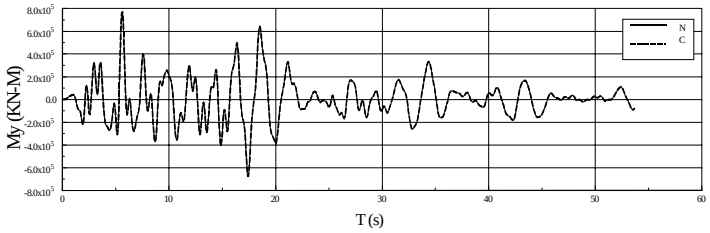

Fig. 6 Time History of M_y

(N: Solution by SAP6 with Added Subroutine, C: Solution by original SAP6)

natural circular frequency ω_1 =0.3893 rad/s and the average of the second and 140th natural circular frequencies $(\omega_2 + \omega_{140})/2$ =5.7557 rad/s are used to determine the Rayleigh damping coefficients, which leads to α_s =0.01458 and β_s =0.006509 for the steel components, and α_c =0.03646 and β_c =0.01627 for the concrete components. The 140th natural period is T_{140}=0.5815 s, which means that the time step 0.02 s for integration is small enough to include the first 140 modes in solution.

The response of the Tsing Ma bridge with non-classical damping to the El Centro three component accelerations are calculated with the methods presented over a time interval of 53.74 s. For comparison, the response of the Tsing Ma bridge, with classical damping ratio 2% and 5%, to these ground accelerations, are calculated with SAP6.

Among the responses, the envelopes of the horizontal moment M_y, vertical moment M_z, torsional moment T_x in the stiffening deck and transverse deformation D_z of the stiffening deck are shown in Figs 7 to10, respectively. The envelopes of the transverse moment M_x, torque T_y and longitudinal deformation D_x of the Ma Wan tower are shown in Figs 11 to 13, with the continuous lines (N) denoting solutions with non-classical damping, the dash-dot lines (S) denoting the solutions with a classical damping ratio of ξ =2%, and the dotted lines(C)denoting the solutions with a classical damping ratio of ξ =5%. These figures show that most of solutions with non-classical damping are in between the two classical damping solutions.

Considering the first 100 modes, [Qin, Luo. and Sun, 1999], the paper analyzes the responses of the Humen bridge to the El Centro three components accelerations. As for the Tsing Ma bridge the Rayleigh damping coefficients are determined as α_s =0.02254 and β_s =0.004026 for the steel components, and α_c =0.05635 and β_c =0.01052 for the concrete components.

The maximum relative differences between solutions for the two bridges with non-classical damping and classical damping calculated as [1-(solution for classical damping) /(solution for a non-classical damping ratio)] are shown in Table 1.

In the table N denotes tensile forces in the main cables of suspension bridges, and torques T_y in towers denote those in the Ma Wan tower for the Tsing Ma bridge and those in the east tower for the Humen bridge.

The analytical results also show that the envelopes of moment M_x and the longitudinal deformation $\boldsymbol{D}_x$ of the Ma Wan tower with non-classical damping are very close to those with classical damping ratio 5%. The transverse deformation $\boldsymbol{D}_z$ of the deck of the Humen bridge with non-classical damping is also close to that with classical damping ratio 2%. However, this deformation with non-classical damping at some position of the deck is a little greater than that with classical damping ratio 2%. The longitudinal moment M_x and the longitudinal deformation $\boldsymbol{D}_x$ of the east tower of the Humen bridge with non-classical damping are close to those with the classical damping ratio 5%.

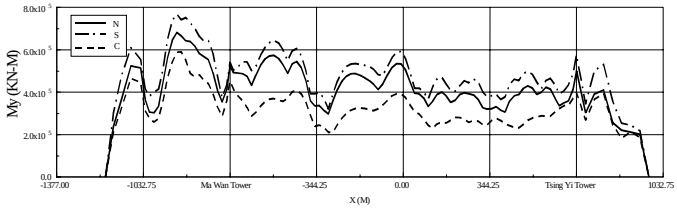

Fig. 7 Envelope of Horizontal Moment M_y in Stiffening Deck of Tsing Ma Bridge

When an average damping ratio of 3.5% is used for classical damping, responses of the steel decks of the two bridges with non-classical damping are greater than those of the decks with classical damping, responses of the

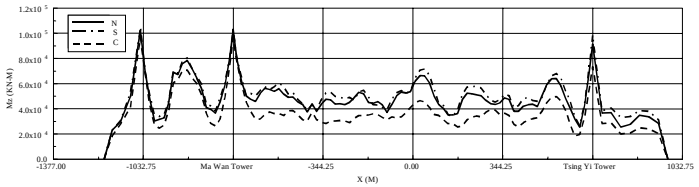

Fig. 8 Envelope of Vertical Moment M_z in Stiffening Deck of Tsing Ma Bridge

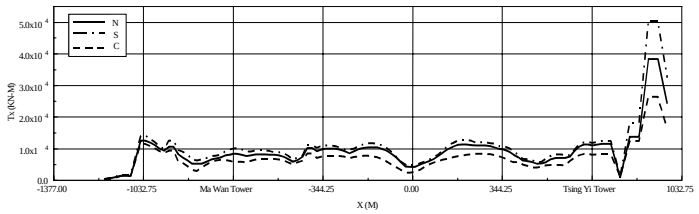

Fig. 9 Envelope of Torque T_x in Stiffening Deck of Tsing Ma Bridge

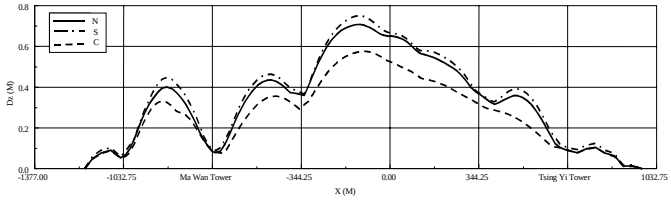

Fig. 10 Envelope of Longitudinal Deformation D_Z of Stiffening Deck of Tsing Ma Bridge

RC towers of the two bridges with non-classical damping, however, are less than those of the towers with classical damping.

In the common practice of civil engineering, it is necessary to consider the difference between the structural response for classical damping ratio 2% and 5%. The analytical responses of the two bridges indicate that the difference between the responses for suspension bridges with non-classical damping and classical damping is at the same order of difference between the responses for classical damping ratio 2% and 5%. Analytical seismic responses with classical damping include significant errors because of the non-classical damping property of long span suspension bridges. On this basis, it can be inferred that the response analysis of suspension bridges to dynamic wind loading should be based on the non-classical damping model.

With Pentium II/266 mHz PC computers, the CPU time for solving the seismic responses of the Tsing Ma bridge with 3211 DOF and with non-classical damping was 3480 s for the step-by-step integration in geometric coordinates; 75 s for step-by-step integration in normal coordinates and 86 s for the pseudo force iteration method. The last two figures do not include the CPU time for solving the eigenequations

CONCLUSIONS

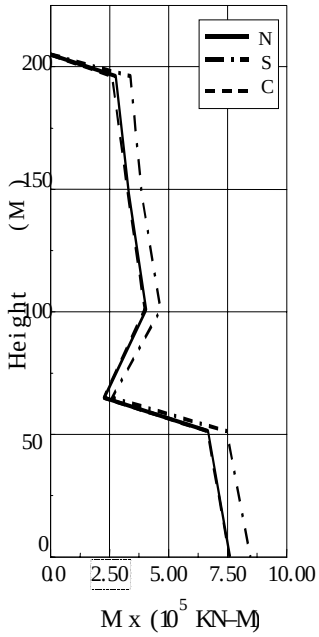

Fig. 11 Envelope of M_x in Ma Wan Tower

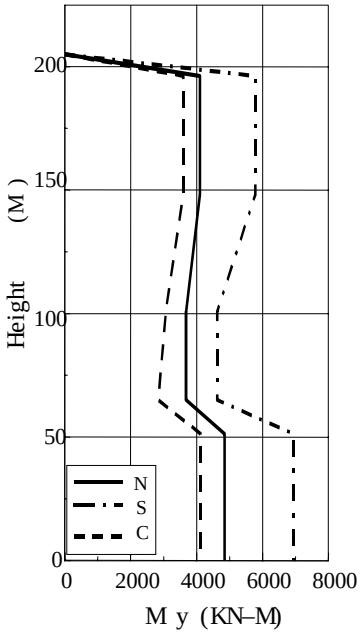

Fig. 12 Envelope of T_y in Ma Wan Tower

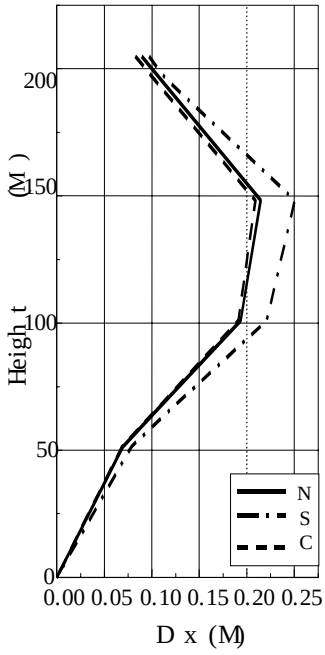

Fig. 13 Envelope of D_x of Ma Wan Tower

Table 1 Maximum Relative Differences between Solutions for Non-classical Damping and Solutions for Classical Damping

	Components of	Tsing Ma Bridge		Humen Bridge	
Deck	M_y	-29%	+36%	-30%	+25%
	M_z	-20%	+36%	-12%	+33%
	T_x	-31%	+31%	-12%	+30%
Tower	T_x	-42%	+23%	-23%	+12%
Main Cables	N	-16%	+9%	-18%	+8%

Three methods for solving the equations of motion with non-classical damping are presented and implemented as computer subroutine. Seismic responses of the Tsing Ma and the Humen bridges with both non-classical damping and classical damping have been analyzed. Comparing results with non-classical damping to those with classical damping shows clear differences. Consequently, the response analysis of suspension bridges to earthquakes and dynamic wind loading should be based on the non-classical damping model.

REFERENCES

Clough R.W. and Penzien J. (1993), *Dynamics of Structures*, McGraw-Hill, Inc., New York.

Caughey T.K. (1960), "Classical Normal Modes in Damped Linear Systems", *Journal of Applied Mechanics*, 27, 4, pp269-271.

Foss K.A. (1958), "Coordinates Which uncouple the Equations of Motion of Damped Linear Dynamic Systems", *Journal of Applied Mechanics*, 32, 4, pp361-364.

Claret A.M. and Venancio-Filho F. (1991), "A Model Superposition Pseudo-Forces Method for Dynamic Analysis of Structural Systems with Non-Proportional Damping", *EESD*, 20, 4, pp303-315.

Ibrahimbegovic A. and Wilson E.L. (1989), "Simple Numerical Algorithms for the Mode Superposition Analysis of Linear Structural Systems with Non-Proportional Damping", *Computers & Structures*, 33, 2, pp523-555.

Qin Q., Luo Y. and Sun H. (1999), "Seismic Analysis of Suspension Bridge Superstructures", *Advances in Structural Engineering*, 2, 2, pp75-85.